

Utility Bounds of Joint Congestion and Medium Access Control for CSMA based Wireless Networks

Tao Wang¹, Zheng Yao¹, Baoxian Zhang¹ and Cheng Li²

¹Research Center of Ubiquitous Sensor Networks
University of Chinese Academy of Sciences
Beijing 100049, China

[e-mail: wangtao13b@mails.ucas.ac.cn, yaozheng@ucas.ac.cn, bxzhang@ucas.ac.cn]

²Faculty of Engineering and Applied Science
Memorial University

St. John's, NL A1B 3X5, Canada
[e-mail: licheng@mun.ca]

*Corresponding author: Baoxian Zhang

*Received May 16, 2016; revised September 9, 2016; accepted October 8, 2016;
published January 31, 2017*

Abstract

In this paper, we study the problem of network utility maximization in a CSMA based multi-hop wireless network. Existing work in this aspect typically adopted continuous time Markov model for performance modelling, which fails to consider the channel conflict impact in actual CSMA networks. To maximize the utility of a CSMA based wireless network with channel conflict, in this paper, we first model its weighted network capacity (i.e., network capacity weighted by link queue length) and then propose a distributed link scheduling algorithm, called CSMA based Maximal-Weight Scheduling (C-MWS), to maximize the weighted network capacity. We derive the upper and lower bounds of network utility based on C-MWS. The derived bounds can help us to tune the C-MWS parameters for C-MWS to work in a distributed wireless network. Simulation results show that the joint optimization based on C-MWS can achieve near-optimal network utility when appropriate algorithm parameters are chosen and also show that the derived utility upper bound is very tight.

Keywords: Network utility maximization, link scheduling, weighted network capacity, joint optimization, multi-path routing

This work was supported in part by the NSF of China under Grant Nos. 61531006, 61471339, 61173158, and the Natural Sciences and Engineering Research Council (NSERC) of Canada (Discovery Grant 293264-12 and Strategic Project Grant STPGP 397491-10).

1. Introduction

Network Utility Maximization (NUM) is an important design consideration for the design of wireless multi-hop networks from both economic and cost perspectives [1][2]. In general, utility is a concept for characterizing the satisfaction or benefit derived by consuming a product or service. Different from the amount consideration when consuming a product or service, utility is usually conformed to the law of diminishing marginal utility, which means that the first unit of consumption of a product or service yields more utility than the second and subsequent units, with a continuing reduction for greater amounts. In a wireless multi-hop network, flow rate (i.e., user bandwidth) is treated as the service provisioned to network users and in this paper we aim to maximize the resulting network utility by optimizing the flow rates assigned to different network users.

By using a utility optimization framework, the NUM can be decomposed into a cross-layered problem, one is congestion control at the transport layer, another is link scheduling at the MAC layer. In the literature, there has been much work in this area including optimization framework designing [3][4][5], link scheduling [6][7][8], and utility modeling [9]. Recently, design of effective cross-layered optimization frameworks has become mature. However, how to achieve efficient link scheduling and maximum utility modeling in a distributed wireless network are still hot research topics.

1.1 Wireless link scheduling

Regarding wireless link scheduling, existing work in this aspect can be roughly categorized into the following three types: back-pressure based, persistence probability based, and CSMA based. In the following, we will introduce typical work belonging to different types, respectively.

The first type adopts the strategy of back-pressure based scheduling and they usually assume that the capacities of wireless links are time-varying [8]. Specifically, at each slot, they work to choose the maximum independent transmission link set, which contains those links leading to the maximum sum of link queue backlog differentials, to transmit data. Due to the NP-Hard nature of the problem, heuristic algorithms (e.g., [10]) were often used for seeking efficient non-conflicting transmission link sets with the assistance of global network state information.

The second type assumes deterministic interference relation among wireless links and they build mathematical models to derive the optimal persistence probability associated with each link for transmissions via cross-layered optimization [6][7]. However, in either of the models in [6][7], medium access operations are purely determined by the statistical persistence probability instead of instantaneous conflict relation among neighbor links as detected via channel sensing. Such operations may even cause more channel conflicts than naive CSMA (Carrier Sensing Multiple Access).

The third type is CSMA and its variants. The naive CSMA purely work at the MAC layer for medium access and it is known to have low performance in multi-hop wireless networks. Recently, how to incorporate various non-MAC-layer factors into CSMA to achieve improved performance has received great attention. In [11], Jiang and Walrand proposed an adaptive CSMA based link scheduling algorithm, which tunes mean back-off time and also mean channel holding time for each link to maximize the global network throughput. In [11], the

authors showed that such a way of link scheduling can yield the maximum possible throughput of a multi-hop wireless network. Adaptive CSMA based link scheduling has the following salient features: It is fully distributed and each node only needs to keep local information; It takes full advantage of channel sensing to relieve potential channel conflict; It can be embedded into a cross-layered optimization to achieve a higher network utility. In [12], Liu et al. extended the work in [11] to achieve total link utility maximization, where link utility is used for describing the scenario where communication pairs are restricted to be direct neighbors.

Since [11], much work has been carried out in the field of adaptive CSMA based link scheduling. Ref. [13] study the scheduling algorithm when the sensing time cannot be negligible. Ref. [14] computes the desired link access intensity (ratio of its mean transmission time to its mean back-off time) for each link when the link is unsaturated. Ref. [15] uses distributed learning mechanism based on game theory for link scheduling in order to achieve total link utility maximization. Ref. [16] studied the impact of channel conflict and proposed an improved version of CSMA by using link activation probability based on queue lengths. For time-varying channels, [17] adjusts the CSMA parameters such as back-off-time and channel holding times, as certain functions of channel capacity, in order to achieve maximal throughput. In [18], the authors studied signal to interference-plus-noise (SINR) based MIMO networks. Among all the above existing work, [14][15] studied networks without conflicts and [13][16][17][18] studied networks with conflicts, [13][14][16][17][18] aimed to maximize network throughput, and [12][15] aimed to maximize total *link* utility. Different from the above work, in this paper, we shall design a link scheduling algorithm that incorporates Adaptive CSMA with cross-layer design, in order to achieve maximum network utility and further we focus on studying networks where peer-to-peer communications via multihop paths are considered and transmission conflicts can occur.

1.2 Utility modeling

Utility modeling of joint (cross-layered) optimization of congestion and medium access control has been an attractive paradigm. Since any layer (including MAC layer) may affect the performance of the joint optimization, utility modeling must work with explicit link scheduling mechanism, in the following, we shall divide existing work in this area based on how link scheduling is performed at the MAC layer.

Existing work in this aspect can again be categorized like those done for addressing the link scheduling issue as introduced in the preceding subsection. For this first type (i.e., back-pressure based), in [9], the authors modeled the network utility in the context of centralized back-pressure based scheduling with the assistance of global network state information. For the second type (i.e., persistence probability based), in [6][7], the authors analyzed the optimality of utility based on the link persistence probability based model, which, however, may cause more channel conflicts. For the third type (i.e., adaptive CSMA based), in [11], the authors analyzed the utility maximization based on adaptive CSMA, and they concluded that the maximal utility can be achieved when parameters such as transmission aggressiveness and algorithm scalar are both infinite. However, in reality, these parameters (or some of them) are not infinite and also they are not independent. That means when one of the parameters has to be chosen to be finite, other parameters will have to be finite as well, which can cause degradation in network utility. Although the authors of [11] further considered the applicability of their continuous-time utility model in scenario with channel conflicts and discrete time, they did not analyze the resulting performance in network utility. In this paper, we shall study the utility modeling based on adaptive CSMA and analyze the impact of various

algorithm parameters with finite values when channel conflict is considered.

Network capacity modeling is also a hot topic that is closely relevant to utility modeling [19]. Thus, a good review of existing work for network capacity modeling can provide good references for studying utility modeling. In this aspect, Ref. [20] builds a model for calculating the capacity of IEEE 802.11 DCF network based on the assumption of conflicts with constant probability and independent probability, respectively. In [21][22], the authors analyzed the capacity of IEEE 802.11 networks when hidden terminals exist. Ref. [23] modified the ideal CSMA model and obtained a product-form stationary distribution incorporating queue length that is associated with the corresponding link delay. Ref. [24] formulated the link capacity when channel sensing fails.

1.3 Our work in this paper

In this paper, we study how to maximize the utility of a CSMA based wireless network with channel conflict. For this purpose, we first model the weighted network capacity of such a network (i.e., network capacity weighted by link queue length), and then propose a distributed CSMA based Maximal-Weight link Scheduling algorithm (C-MWS) to maximize the weighted network capacity. We deduce the utility upper and lower bounds based on the weighted network capacity model and analyze the impact of various parameters, where the utility bounds can help network operator/users to learn the maximal network capacity and evaluate the effectiveness of an network optimization algorithm.

Our work in this paper is based on the following assumptions, which were also used in [11][25][26]: 1) there exist no hidden nodes in the network; 2) channel sensing is instantaneous. One way of resolving the issue of hidden nodes is to use separate signaling channel for medium access control and resource allocation decision making. In addition, we assume that the network under study is saturated.

The major contributions in this paper are listed as follows.

- 1) We model the weighted network capacity for a wireless network with channel conflicts and then present the design of C-MWS to maximize the weighted network capacity.
- 2) We build a mathematical model to derive the utility upper and lower bounds via joint optimization of congestion control and link scheduling based on C-MWS. Through this model, we can learn how the C-MWS parameters affect the network utility and also how to tune them to improve the network utility.
- 3) Simulation results show that the joint optimization based on C-MWS can achieve near-optimal network utility when appropriate algorithm parameters are chosen and also show that the derived utility upper bound is very tight.

The rest of the paper is structured as below. Section 2 gives system model and then deduces the joint optimization structure. Section 3 models the weighted network capacity and proposes the C-MWS algorithm for achieving the weighted network capacity. Section 4 derives the utility bounds and analyzes the network stability. Section 5 presents simulation results for performance evaluation. Finally, in Section 6, we conclude this paper.

2. System Model

In this section, we focus on studying wireless multi-hop networks, which can be modeled by a directed graph $\mathcal{G}=(\mathcal{N}, \mathcal{L})$, where \mathcal{N} represents the set of nodes and \mathcal{L} represents the set of directional links connecting nodes in the graph. $l(m, n) \in \mathcal{L}(\mathcal{G})$ means that there exist a link from node $m \in \mathcal{N}(\mathcal{G})$ to its neighbor node $n \in \mathcal{N}(\mathcal{G}) - \{m\}$. Notations used in the rest of this paper are

listed in **Table 1**.

Next, we adopt a widely used interference model in our study, which can be described as follows. It is realistic to assume that a node $n \in \mathcal{N}(\mathcal{G})$ cannot transmit traffic while any other node within its sensing range is transmitting. The directed graph \mathcal{G} is associated with a unidirectional conflict graph $\mathcal{CG}=(\mathcal{V}, \mathcal{E})$, where each node in \mathcal{CG} represents a link in the original graph \mathcal{G} , and each link in \mathcal{CG} represents a symmetric interference relation. For example, $v_1, v_2 \in \mathcal{V}(\mathcal{CG})$ are neighbor vertices and $e(v_1, v_2) \in \mathcal{E}(\mathcal{CG})$ is the edge connecting v_1 and v_2 . The existence of such a link represents that the two links that v_1 and v_2 represent in the original graph interfere with each other. In addition, for a link $l(m, n) \in \mathcal{L}(\mathcal{G})$, let $C_{l,\max}$ represent its theoretical maximum capacity when it is not interfered by any other link and external environment.

Table 1. NOTATIONS.

Notations	Definitions
$\mathcal{G}=(\mathcal{N}, \mathcal{L})$	The original graph;
$ \mathcal{L} $	Number of links in the original graph;
$\mathcal{CG}=(\mathcal{V}, \mathcal{E})$	Conflict graph of the original graph \mathcal{G} ;
$x_r^s; x_r^{s(opt)}; x_r^{s(*)}$	Flow rate; flow rate by centralized optimal scheduling; an arbitrary flow rate by C-MWS. All these variables are for a sub-path r for session s ;
$p_l; p_l^{(opt)}$	The Lagrange Multiplier (also called weight) and the optimal Lagrange Multiplier obtained by centralized scheduling for link l , respectively;
$c_l; c_l^{(opt)}; c_l^{(*)}; c_l^{(e)}$	Link rate, optimal link rate by centralized scheduling, stationary link rate by C-MWS, and empirical link rate by C-MWS. All are for link l ;
$C_{l,\max}$	Theoretical maximal link capacity for link l ;
$\gamma_r; \gamma_l$	Joint optimized flow rate and queue step size for a sub-flow r ;
$1/\delta_l; 1/\mu_l$	Mean back-off time and transmission time for link l ;
T	Duration of scheduling cycle;
τ	Duration of a mini timeslot for channel access;
$is; is'; iss$	All are independent sets. is' and is represent a pair of left and right states, respectively, where the right one has one more extra link l ;
P_{is}	Fraction of time when the network under study is in state is ;
$P_{S_{is}^l}$	Probability that a packet is successfully transmitted over link l when the network state is is ;
α	A scalar for the C-MWS algorithm;
$\overline{CW}_{\min}; \overline{CW}_{\max}$	Minimal mean contention window size (\overline{CW}); maximal \overline{CW} ;
BF_l	Back-off time (which is integer multiple of a mini timeslot) for packet transmission over link l ;
$r_l; r_{\min}; r_{\max}$	Transmission Aggressiveness (TA) for link l ; minimal TA; maximal TA;
$\mathcal{NC}; \mathcal{ENC}; \mathcal{PNC}$	Network capacity without conflict; network capacity with conflict; weighted network capacity;

$x_{\max}; U_{\max}$	Upper bound of x_r^s ($\forall r, s$) and $U_s(x^s)$ ($\forall s$);
$L_{\max}; f_{\max}$	The number of links in the longest path among all the sub-paths by different sessions; maximal number of flows traversing a link;
$\Delta \mathcal{A}(\mathbf{p}, r_{\max}, r_{\max}, \alpha)$	Difference between the optimal weighted network capacity by centralized scheduling and that by our C-MWS algorithm;
$\Delta \mathcal{B}$	Analytical deviation due to approximation of Lagrange Multiplier;
$\Delta \mathcal{C}$	Deviation in network capacity due to non-ideal steady implementation in each scheduling cycle;
$\Delta \mathcal{D}$	Analytical deviation due to cumulative steady state error.

In this paper, CSMA-based back-off process is performed by using a counter with memory function. Specifically, a link l that has traffic to transmit will generate an integer $BF_l = \lfloor T_{l,bc} / \tau \rfloor$ which represents the number of mini-timeslots (MTS), denoted by τ , for backoff in channel access; $T_{l,bc}$ is a variable representing the back-off time that link l chooses for its next transmission and it is exponentially distributed with mean of $E[T_{l,bc}]$, satisfying $\overline{CW}_l = \lfloor E[T_{l,bc}] / \tau \rfloor$, where \overline{CW}_l represents the mean contention window size for link l . Each link can sense the channel state (idle or busy) only at the beginning of a mini-timeslot: If the channel is idle, the link l starts a countdown process based on the current counter. When the counter reaches zero, the link l initializes a transmission; If the channel is busy during the countdown process of link l , the counter is frozen. The countdown process re-starts after link l senses the channel is idle.

Let $s \in \mathcal{S}$ denote a traffic session with flow rate x^s , where \mathcal{S} denotes the set of traffic sessions in the network. Each session may take multiple paths from the session source to the destination. Let r/s denote the set of all sub-paths for a session $s \in \mathcal{S}$, each of which transmits part of the traffic for the session. Let x_r^s denote the flow rate for session s on sub-path r , satisfying $\sum_{r/s} x_r^s = x^s$, which is the aggregated rate of all the sub-paths belonging to session $s \in \mathcal{S}$. $U_s(x^s)$ is the utility associated with session s . The utility function $U_s(\cdot)$ is assumed to be twice differential, strictly concave, and non-decreasing with mean flow rate.

Accordingly, the joint optimization problem of link scheduling at the MAC layer and end-to-end congestion control at the transport layer for achieving network utility maximization can be brought together as follows:

$$\begin{aligned}
& \max_{x_r^s} \sum_{s \in \mathcal{S}} U_s(x^s) \\
& \text{s.t.} \quad \sum_{r/l} x_r^s \leq c_l \quad \forall l \\
& \quad \quad \pi_l C_{l,\max} = c_l \quad \forall l
\end{aligned} \tag{1}$$

where π_l and c_l denote the link transmission probability and link rate, respectively, and r/l is a set containing all the sub-paths passing through link $l \in \mathcal{L}$. The link rate c_l is the maximum rate at which data packets are allowed to be transmitted through link l during the current scheduling cycle as returned by a link scheduling algorithm. In this sense, in this paper, we also treat c_l as the capacity of link l . The first constraint in (1) is the rate capacity constraint for each link. The second is the link scheduling constraint for link transmission probability of each link.

By relaxing the capacity constraint in (1), we have (still subject to the second constraint):

$$\begin{aligned}
L(x, p) &= \sum_s U_s(x^s) - \sum_l p_l \left(\sum_{r|l} x_r^s - c_l \right) \\
&= \sum_s (U_s(x^s) - \sum_{r|s} q_r x_r^s) + \sum_l p_l c_l
\end{aligned} \tag{2}$$

where p_l is the Lagrange multiplier, which can be interpreted as the queue size for link l . We define $q_r = \sum_{l|r} p_l$, which denotes the sum of queue backlogs on all the links belonging to sub-path r . In the second line of (2), it should be noted that the first term is separable in x_r^s , and the second term is separable in c_l . Thus, the objective function of the dual problem is as follows:

$$D(x) = \max_{p \geq 0} L(x, p) = \sum_s V_s + W$$

where

$$V_s = \max_{x_r^s} (U_s(x^s) - \sum_{r|s} q_r x_r^s) \tag{3a}$$

$$W = \max_{c_l} \sum_l p_l c_l \quad s.t. \quad \pi_l C_{l, \max} = c_l, \quad \forall l. \tag{3b}$$

The sub-problems (3a) and (3b) can be realized by flow control and MAC layer scheduling, respectively, which are coupled by the Lagrange multiplier p . Specifically, (3a) shows that the source node of each session should generate its traffic at a rate to maximize its own profit that is the difference between its achieved utility and the cost spent for the corresponding bandwidth usage. (3b) shows that all links should try to maximize the weighted network capacity (i.e., network capacity weighted by p_l) under the condition of equilibrium of network queues. In other words, in (3b), the network maximizes its weighted network capacity subject to the constraint that a link has higher priority of transmission when its link queue backlog is larger than those on its neighbor links for mitigating network congestion. For simplicity of representation, hereafter, the terms ‘‘Lagrange multiplier’’ and ‘‘weight’’ will be used interchangeably unless otherwise stated. Thus, the joint optimization problem in (3) can be interpreted in a way such that a network tries to obtain the flow rate that makes the global profit maximum, under the condition that the weighted network capacity is maximal.

The flow control sub-problem (3a) can be easily solved by using the following gradient descent method.

$$\dot{x}_r^s[(n+1)T] = \gamma_r (U_s'(x^s(nT)) - q_r(nT))_{x_r^s(nT)}^+ \tag{4}$$

where $\gamma_r > 0$ is flow rate step size, T denotes the duration of scheduling cycle, and $(\cdot)_v^+$ is a positive projection, which verifies $(\cdot)_v^+ = 0$ whenever $v \leq 0$, or otherwise $(\cdot)_v^+ = \cdot$.

For the MAC scheduling control sub-problem (3b), the function $\max \sum_{l|r} p_l c_l$ is not strictly concave, so it is difficult to obtain its optimal solution. Here, we adopt a fully CSMA based distributed algorithm for obtaining approximate solution. The algorithm details can be found in Section 3.

In each iteration of the joint optimization, the Lagrange multiplier gradient is updated as follows:

$$\dot{p}_l[(n+1)T] = \gamma_l \left(\sum_{r|l} x_r^s(nT) - c_l^{(e)}(nT) \right)_{p_l(nT)}^+ \tag{5}$$

where $\gamma_l > 0$ is queue step size. At the beginning of each scheduling cycle, we calculate the average empirical link rate $c_l^{(e)}$ for each link l for the link to transmit traffic. Thus, the Lagrange multiplier updating process reflects the change in link load over time.

3. Weighted Network Capacity Model and C-MWS Algorithm

From the preceding section, we can see that solving the sub-problem of weighted network capacity in (3b) is the key for solving the joint optimization problem. Furthermore, it will be seen in Section 4 that weighted network capacity is directly correlated to the ultimate network utility. In this section, we shall model the weighted network capacity and then present the design of C-MWS algorithm for pursuing maximal weighted network capacity. Specifically, we will first describe how to model the weighted capacity of a network without conflict, and then extend the result to weighted network capacity for networks with channel conflict. Finally, by using the derived network capacity, we propose the C-MWS algorithm.

3.1 Modeling of network capacity without conflict

In this subsection, we start from the modeling of network capacity, and then extend the results to weighted network capacity without conflict and analyze its characteristics. In here, we assume that $C_{l,\max} (\forall l)$ are identical and are normalized to 1.

1) Network capacity without conflict

Network capacity without channel conflict have been studied in [11][25][26]. For the integration of description, we introduce their results in the following.

Let \mathcal{IS} denote all the independent sets whose links can transmit simultaneously without conflict. Assume that a state $is' \in \mathcal{IS}$ has n links, and state $is \in \mathcal{IS}$ contains an additional link l besides the n links in state is' . In other words, $is, is' \in \mathcal{IS}$ can be seen as a pair of right and left states, where the right state contains exactly one more link than the left one.

Table 2. Operator Notations.

Notations	Definitions
$\sum_{is} f(\cdot); \sum_{iss} f(\cdot)$	Sum of $f(\cdot)$ for all states, $is, iss \in \mathcal{IS}$. $f(\cdot)$ is a function that characterizes a specific property of a state.
$\sum_{l is} f(\cdot)$	Sum of $f(\cdot)$ for all links belonging to state is ;
$\sum_{is l} f(\cdot)$	Sum of $f(\cdot)$ for all states that contain link l ;
$\sum_{\bar{is} l} f(\cdot)$	Sum of $f(\cdot)$ for all states that do not contain link l .

Let $1/\delta_l = E[T_{l,bc}]$ and $1/\mu_l = E[T_{l,tr}]$, where $T_{l,tr}$ represents the transmission time for each packet transmission over link l . Furthermore, we assume that the distribution of $T_{l,bc}$ is exponential. Thus, the state transition from is' to is happens at rate δ_l , and the state transition from is to is' happens at rate μ_l . Since all the states in \mathcal{IS} form a continuous time Markov chain and the detailed balance equations hold [27]. That is, $\theta_l = \mu_l / \delta_l$ represents the link transition rate for link l . Let P_{is} represent the fraction of time when the network stays in state is . We have

$$P_{is} = \frac{1}{\theta_l} P_{is'}. \quad (6)$$

For simplicity of exposition, let $\exp(r_l) = \theta_l$, where r_l is the ‘‘transmission aggressiveness’’ (TA) of link l [11]. Some operator notations used later are further summarized in Table 2.

For a given TA vector $\mathbf{r} = \{r_1, r_2, r_3, \dots, r_{|\mathcal{L}|}\}$, where $|\mathcal{L}|$ is the total number of links in the

original network, by using the time-reversibility of Markov process, the stationary distribution of P_{is} ($\forall is$) can be characterized as follows [25][26]:

$$P_{is} = \frac{\exp(\sum_{l|is} r_l)}{\sum_{iss} \exp(\sum_{l'|iss} r_{l'})}, \quad (7)$$

where the summation \sum_{iss} is over all feasible states in \mathcal{IS} , and $\sum_{l|is}$ denotes the summation over all the links belonging to state is . Based on the above results, we can see that the network capacity can be calculated by the sum of the *attainable* capacities of all links and the attainable capacity of a link l equals to the sum of the fraction of time of all states that contain the link. That is, the network capacity can be calculated as follows:

$$\mathcal{NC}(\mathbf{r}) = \sum_l (\sum_{is|l} P_{is}), \quad (8)$$

where the summation $\sum_{is|l}$ is over all feasible states, which contain link l . Substituting (7) into (8), we can obtain the network capacity $\mathcal{NC}(\mathbf{r})$ as follows:

$$\mathcal{NC}(\mathbf{r}) = \frac{\sum_{is} K_{is} \exp(\sum_{l|is} r_l)}{\sum_{iss} \exp(\sum_{l'|iss} r_{l'})} \quad (9)$$

where K_{is} denotes the number of links in state is .

2) Weighted network capacity without conflict

Now, we go back to the optimization objective in (3b). We assume a weight vector $\mathbf{p} = \{p_1, p_2, p_3, \dots, p_{|\mathcal{L}|}\}$, where p_l is the weight associated with link l , $1 \leq l \leq |\mathcal{L}|$. According to (9), we deduce the weighted network capacity $\mathcal{NC}(\mathbf{p}, \mathbf{r})$ as follows:

$$\mathcal{NC}(\mathbf{p}, \mathbf{r}) = \frac{\sum_{is} W_{is} \exp(\sum_{l|is} r_l)}{\sum_{iss} \exp(\sum_{l'|iss} r_{l'})}, \quad (10)$$

where $W_{is} = \sum_{l|is} p_l$ denotes the sum of the weights of all links in state is . In order to inspect how a particular link affects the weighted network capacity, we present the following proposition.

Proposition 1: Assume that the TA associated with a link l , r_l is adjustable. Then, we have that the weighted network capacity by (10) increases with r_l as $r_l \rightarrow +\infty$, when the link l satisfies the following condition.

$$\frac{\sum_{is|l} W_{is} \exp(\sum_{l'|is} r_{l'})}{\sum_{is|l} \exp(\sum_{l'|is} r_{l'})} \geq \frac{\sum_{\bar{is}|l} K_{\bar{is}} \exp(\sum_{l'|is} r_{l'})}{\sum_{\bar{is}|l} \exp(\sum_{l'|is} r_{l'})}, \quad (11)$$

where the summation $\sum_{\bar{is}|l}(\cdot)$ is over all feasible states that do not contain link l . Otherwise, the network capacity by (10) decreases with r_l as $r_l \rightarrow +\infty$.

Proof: We increase r_l by β ($\beta \geq 0$) for the link l . Accordingly, the change in the weighted network capacity will be as follows.

$$\frac{\sum_{is|l} \{(\sum_{l'|is} p_{l'}) \exp(\sum_{l'|is} r_{l'} + \beta)\} + \sum_{\bar{is}|l} \{(\sum_{l'|is} p_{l'}) \exp(\sum_{l'|is} r_{l'})\}}{\sum_{is|l} \exp(\sum_{l'|is} r_{l'} + \beta) + \sum_{\bar{is}|l} \exp(\sum_{l'|is} r_{l'})} - \frac{\sum_{is} \{(\sum_{l'|is} p_{l'}) \exp(\sum_{l'|is} r_{l'})\}}{\sum_{is|l} \exp(\sum_{l'|is} r_{l'}) + \sum_{\bar{is}|l} \exp(\sum_{l'|is} r_{l'})} \quad (12)$$

Here, to ease the description, we use ω , $\omega \geq 1$, to represent $\exp(\beta)$. Transform the above expression to a common denominator by directly multiplying the two denominators, the corresponding numerator will become the following.

$$(\omega - 1) \left(\sum_{is|l} W_{is} \exp\left(\sum_{l'|is} r_{l'}\right) \right) \left(\sum_{is|l} \exp\left(\sum_{l''|is} r_{l''}\right) \right) - \left(\sum_{is|l} W_{is} \exp\left(\sum_{l''|is} r_{l''}\right) \right) \left(\sum_{is|l} \exp\left(\sum_{l'|is} r_{l'}\right) \right) \quad (13)$$

It can be easily derived when the above expression is greater than 0, (10) increases as r_l increasing. In addition, we calculate the derivative of (13) over ω , it can be seen that (12) monotonely increases with ω , which means (10) increases with r_l as $r_l \rightarrow +\infty$. Otherwise, when $\beta < 0$, it can be seen that $\omega < 1$. Thus, (10) decreases with r_l as $r_l \rightarrow -\infty$. So (11) follows. ■

Proposition 1 also reveals a clear correlation between weighted network capacity and the range of link TA. Suppose $r_{\min} \leq r_l \leq r_{\max}$ ($\forall l$), the *attainable* maximal weighted network capacity is positively correlated to r_{\max} for a fixed r_{\min} . That is, the larger r_{\max} is, the larger the attainable maximal weighted network capacity will be, provided that there exist no transmission conflict in the network.

3.2 Modeling of weighted network capacity with conflicts

The model in the preceding subsection, however, is not suitable for real CSMA networks. In the above model, back-off time is assumed to be continuous, while the back-off time in real CSMA networks is slotted and it is an integer multiple of *MTS*.

Due to the time reversibility of CSMA Markov chain, (7) is an equally valid expression for different distributions of back-off time [21][26]. Thus, it can be seen that when back-off time is integer, (7) is still valid. We again assume that $is, is' \in \mathcal{IS}$ are a pair of right and left states, respectively, where the right state contains exactly one more link l than the left one. When the network time is slotted, a link l may be activated simultaneously with one of its interfering links (say l') after its backoff counter drops to zero. If the effect of link conflict by l' was ignored, the state transition probability from is' to is ($is' \cup l$) would be consistent with (6); If so, the state transition probability from is ($is' \cup l$) to state is' would also be consistent with (6). In that case, (7) would also be valid for a discrete-time CSMA network. However, the truth is that transmission conflict can happen in a discrete-time network.

The capacity of a state is is the sum of effective link rates of all the links in the state. Thus, the weighted capacity of a network with transmission conflict, denoted by $\mathcal{E}\mathcal{N}\mathcal{C}(\mathbf{p}, \mathbf{r})$, can be expressed as the sum of the capacity of all its states as follows.

$$\mathcal{E}\mathcal{N}\mathcal{C}(\mathbf{p}, \mathbf{r}) = \sum_{is} W_{is} \left(\sum_{l|is} P_{is} \text{Ps}_{is}^l \right), \quad (14)$$

where Ps_{is}^l is the probability that a packet is successfully sent over the link l when the network state is is .

Let us again focus on a pair of states $is, is' \in \mathcal{IS}$. In the continuous time Markov model, after the activation of link l , the network state changes from is' to is . Thus, Ps_{is}^l is the sum of all the probabilities for link l to take all possible back-off time m ($\forall m$) for successful transmissions when the network works in state is ($is' \cup l$). Specifically, when back-off time BF_l of link l picks an integer m , the link l can successfully transmit data when the BF value of any other link conflicting with link l does not pick the same integer. Thus, we have

$$\text{Ps}_{is}^l = \sum_{m=0}^{+\infty} \text{P}\{BF_l = m\} \prod_{l'|l} (1 - \text{P}\{BF_{l'} = m\}) \quad (15)$$

where l'/l denotes a set of all the links, each of which conflicts with link l but not any link in is' .

Since the back-off time $T_{l, bc}$ is assumed to be exponentially distributed with $E[T_{l, bc}] = 1/\delta_l$

and further time is slotted, link l picks the integer $BF_l = \lfloor T_{l,bc}/\tau \rfloor$ when the back-off time picks the value $T_{l,bc}$. Therefore, the probability at which BF_l equals to integer m is as follows.

$$P\{BF_l = m\} = \exp(-\delta_l \tau m) - \exp(-\delta_l \tau (m+1)), \quad \forall l \quad (16)$$

Let \overline{CW}_{\min} (resp., \overline{CW}_{\max}) is the minimal (resp., maximal) mean contention window size. The introduction of \overline{CW}_{\min} and \overline{CW}_{\max} in this paper is partially motivated by the IEEE 802.11 standards, where minimal and maximal contention window sizes for medium access are used to control the channel conflict and delay for each transmission. The differences are that here we use the mean value instead of absolute value and use exponentially distribution instead of uniform distribution.

Assume $r_{\min} \leq r_l \leq r_{\max}$ ($\forall l$), r_{\min} is fixed, and r_{\max} is adjustable. Suppose Proposition 1 still holds, the maximal *attainable* weighted network capacity would increase as r_{\max} increasing. However, larger r_{\max} also means smaller \overline{CW}_{\min} , and decrease of \overline{CW}_{\min} will cause more conflicts in the network and thus degradation in the maximal attainable weighted network capacity. Thus, it is rational to conclude that there must exist an optimal r_{\max} (correspondingly optimal \overline{CW}_{\min}) that maximizes (14).

To this end, we can derive the weighted network capacity as defined in (3b) by using (14) via centralized scheduling. However, in reality, even given r_{\min} and r_{\max} , it is still difficult to determine the optimal TA for each link in a distributed manner. Next, we will present a distributed link scheduling algorithm C-MWS.

3.3 C-MWS algorithm

Before presenting the detailed link scheduling algorithm, we firstly discuss the importance of introducing r_{\max} (resp., \overline{CW}_{\min}) and r_{\min} (resp., \overline{CW}_{\max}).

For given mean transmission time, larger TA means smaller mean back-off time. Smaller mean back-off time means increase of channel conflict. Thus, how to set the upper bound of TA has critical impact on the performance of an interfering network. On the other hand, as the mean back-off time increases, the waste of channel resource increases. Thus, the TA also needs a lower bound. In C-MWS, each link (say l) in the network independently calculates its TA value based on its weight p_l . Intuitively, given lower and upper bounds r_{\min} (resp., \overline{CW}_{\max}) and r_{\max} (resp., \overline{CW}_{\min}), link l should have higher probability to transmit when it has larger weight p_l . Accordingly, for a link l , its TA for the next scheduling cycle is calculated as follows.

$$r_l(p_l) = \begin{cases} r_{\min} + \alpha p_l & r_{\min} + \alpha p_l < r_{\max} \\ r_{\max} & r_{\min} + \alpha p_l \geq r_{\max} \end{cases}, \quad \forall l \quad (17)$$

where α is a scalar. By substituting (7), (15), (16), and (17) into (14), we can obtain a weighted network capacity. (17) is the core of C-MWS based link scheduling and how it works will be presented in following subsection 3.5. For simplicity of presentation, hereafter, r_{\max} (resp., \overline{CW}_{\min}), r_{\min} (resp., \overline{CW}_{\max}), and α altogether will also be called C-MWS parameters.

Through extensive simulation results, we find that the weighted network capacity by (14) is non-monotonous over the above C-MWS parameters. Thus, different C-MWS parameters can lead to different weighted network capacities.

Due to the introduction of the C-MWS parameters, the difference between the optimal solution by centralized scheduling and that by C-MWS can be calculated as follows.

$$\Delta \mathcal{A}(\mathbf{p}, r_{\min}, r_{\max}, \alpha) = p_{is, \max} - \mathcal{E} \mathcal{N} \mathcal{C}(\mathbf{p}, r_{\min}, r_{\max}, \alpha) \quad (18)$$

where $p_{is, \max} = \max_{is \in \mathcal{I}^S} (\sum_{l \in \mathcal{I}^S} p_l)$ denotes the maximal state weight among all the states and the

weight of a state is the sum of the link weights associated with all the links belonging to the state.

3.4 Impact of duration of scheduling cycle

According to [11], given finite TA, the stationary distribution of transmission probability will maximize the network capacity as time evolves. Thus, the duration of scheduling cycle affects the network capacity. The convergence time of CSMA Markov chain is bounded as follows [28].

$$|s_l^{(e)} - s_l^{(*)}| \leq \frac{C}{T} \quad (19)$$

where C is a network parameter, which is a constant depending on the network scale and r_{\max} , T is duration of a scheduling cycle, $s_l^{(e)}$ is the empirical service rate, and $s_l^{(*)}$ is the stationary service rate. Then, the difference between weighted service rate for infinite time and that for finite T can be obtained as follows.

$$\sum_l p_l s_l^{(e)} \geq \sum_l p_l s_l^{(*)} - \frac{C}{T} \sum_l p_l \quad (20)$$

3.5 C-MWS implementation

C-MWS works as follows. Each link l in the network uses its TA value r_l returned by (17) to calculate its mean back-off time $E[T_{l,bc}]$, based on which the link generates its back-off time BF_l for transmitting each packet. Furthermore, each link needs to count the number of already-served packets over the link in the current scheduling cycle. Equation (21) establishes a bridge between C-MWS and the objective in (3b).

$$c_l^{(e)} = s_l^{(e)} \quad (21)$$

3.6 Achievable bounds of weighted network capacity

In order to analyze the utility bound of the joint optimization problem (1), we first need to know the bounds of weighted network capacity by C-MWS in each scheduling cycle. Regarding this, we have the following proposition.

Proposition 2: The empirical weighted network capacity $W^{C-MWS} = \sum_l p_l c_l^{(e)}$ resulted by (22) is bounded. In particular

$$W^* - \Delta\mathcal{C}(T) \leq W^{C-MWS} \leq W^{opt} - \Delta\mathcal{A}(\mathbf{p}, r_{\min}, r_{\max}, \alpha) \quad (22)$$

where $W^* = \sum_l p_l c_l^{(*)}$ denotes the stationary weighted network capacity based on C-MWS for given link weights; $W^{opt} = \sum_l p_l c_l^{(opt)}$ denotes the optimal weighted network capacity by centralized scheduling; $\Delta\mathcal{C}(T) = (C/T) \sum_l p_l$.

Proof: Since $c_l^{(*)}$ is the stationary link rate, according to (18), we have $W^{opt} - W^* = \Delta\mathcal{A}(\mathbf{p}, r_{\min}, r_{\max}, \alpha)$. According to (20), we have $W^{C-MWS} \geq W^* - \Delta\mathcal{C}(T)$. In addition, $W^{C-MWS} \leq W^*$. So (22) follows. ■

4. Network Stability and Utility Bounds

In the preceding section, we have modelled the weighted network capacity and deduced its achievable bounds based on C-MWS. Next, we will introduce these results into the analysis of the joint optimization problem defined in (1). It is necessary to define the notation of stability

before analysis.

Definition 1 [3][9]: A network is stable in the mean or simply stable if

$$\limsup_{M \rightarrow +\infty} \frac{1}{M} \sum_{\tau=1}^M E[p_l(\tau T)] < \infty \quad (23)$$

over joint optimization cycles $\{1, 2, 3, \dots, M\}$, where M is a positive integer. In addition, it is easy to derive that a sub-path flow rate x_r^s has non-tight upper bound x_{\max} , i.e., $x_r^s \leq x_{\max}$. To analyze the utility and stability of the joint optimization, we firstly introduce a Lyapunov drift with utility function that enables our analysis to be decomposed into the congestion and scheduling control sub-problems.

4.1 Lyapunov drift with utility

Define the Lyapunov function $L(\mathbf{p}[kT]) = \sum_l p_l^2[kT]$. Then, define the conditional Lyapunov drift $\Delta L(\mathbf{p}[kT])$ as follows [3][7].

$$\Delta L(\mathbf{p}[kT]) = \{L(\mathbf{p}[(k+1)T]) - L(\mathbf{p}[kT]) | \mathbf{p}[kT]\} \quad (24)$$

where the conditional expectation is in terms of the Lagrange multiplier dynamics based on (5).

Substitute the $p_l[(k+1)T]$ item in (24) by (5), we have

$$\begin{aligned} \Delta L(\mathbf{p}[kT]) &= E\left\{\sum_l p_l^2[(k+1)T] - \sum_l p_l^2[kT] | \mathbf{p}[kT]\right\} \\ &= E\left\{2\sum_l \gamma_l p_l[kT] \left(\sum_{r|l} x_r^s[kT] - c_l^{(e)}\right) | \mathbf{p}[kT]\right\} + E\left\{\sum_l \dot{p}_l^2[kT] | \mathbf{p}[kT]\right\} \end{aligned}$$

Since $E\{\dot{p}_l^2[kT]\} \leq (\gamma_l f_{\max} x_{\max})^2$, where f_{\max} denotes the maximal number of flows that traverses a link, we have

$$\Delta L(\mathbf{p}[kT]) \leq \Delta \mathcal{B} + E\left\{2\sum_l \gamma_l p_l[kT] \sum_{r|l} x_r^s[kT] | \mathbf{p}[kT]\right\} - E\left\{2\sum_l \gamma_l p_l[kT] c_l^{(e)}[kT] | \mathbf{p}[kT]\right\} \quad (25)$$

where $\Delta \mathcal{B} = L_{\max} (\gamma_l f_{\max} x_{\max})^2$, L_{\max} represents the maximal number of links that have traffic to transmit for different sub-paths.

Subtracting the expression $2\gamma_l E\{\sum_s U_s(x^s[kT]) | \mathbf{p}[kT]\}$ from both sides of (25), we have

$$\begin{aligned} &\Delta L(\mathbf{p}[kT]) - 2\gamma_l E\left\{\sum_s U_s(x^s[kT]) | \mathbf{p}[kT]\right\} \\ &\leq 2E\left\{\gamma_l \sum_s U_s(x^s[kT]) - \sum_r \sum_{l|r} \gamma_l p_l[kT] x_r^s[kT] | \mathbf{p}[kT]\right\} - E\left\{2\sum_l \gamma_l p_l[kT] c_l^{(e)}[kT] | \mathbf{p}[kT]\right\} + \Delta \mathcal{B} \\ &\leq 2\gamma_l \psi(\mathbf{p}[kT]) - 2\gamma_l \phi(\mathbf{p}[kT]) + \Delta \mathcal{B} \end{aligned} \quad (26)$$

where $\psi(\mathbf{p}[kT])$ and $\phi(\mathbf{p}[kT])$ denote the flow rate function and the MAC scheduling control function, respectively. Specifically,

$$\psi(\mathbf{p}[kT]) = E\left\{\sum_s U_s(x^s[kT]) - \sum_r \sum_{l|r} p_l[kT] x_r^s[kT] | \mathbf{p}[kT]\right\} \quad (27a)$$

$$\phi(\mathbf{p}[kT]) = E\left\{\sum_l p_l[kT] c_l^{(e)}[kT] | \mathbf{p}[kT]\right\} \quad (27b)$$

Since (27a) is a standard expression in previous work [2][6], the sub-gradient algorithm function (4) can solve the flow rate control function $\psi(\mathbf{p}[kT])$. In the meantime, the scheduling control function $\phi(\mathbf{p}[kT])$ is solved by C-MWS.

4.2 Network stability and utility bounds

To analyze the utility and stability of the joint optimization, the following three lemmas are presented.

Lemma 1: Let $x_r^{s(*)}$ denote an arbitrary flow rate for sub-path r of session s (subject to (1)), then, the cumulative flow rate control function over joint optimization cycles $\{1, 2, 3, \dots, M\}$ satisfies

$$\sum_{\tau=1}^M \{\psi(\mathbf{p}[\tau T])\} \geq M \sum_s U_s(x^{s(*)}) - \sum_{\tau=1}^M \sum_r \sum_{l/r} p_l[\tau T] x_r^{s(*)} + \Delta \mathcal{D} \quad (28)$$

where $\Delta \mathcal{D} = -\sum_r \eta_r x_r^{s(*)} (x_r^s[MT] - x_r^s[T])$, $\eta_r = (1/\gamma_r + U_{s,\min}'') > 0$. $U_{s,\min}''$ is the minimal value of $U_s''(x^s)$.

Proof: We first calculate the following expression

$$\Delta \psi(\mathbf{p}[kT]) = \psi(\mathbf{p}[kT]) - E\left\{ \left(\sum_s U_s(x^{s(*)}) - \sum_r \sum_{l/r} p_l[kT] x_r^{s(*)} \right) \middle| \mathbf{p}[kT] \right\}.$$

Taking expectation over $\mathbf{p}[kT]$ for $\Delta \psi(\mathbf{p}[kT])$ and using the Lagrange mean value theorem for the first term of the expression in the following line, we have

$$\begin{aligned} & \sum_s (U_s(x^s[kT]) - U_s(x^{s(*)})) + \sum_r q_r[kT] (x_r^{s(*)} - x_r^{s(*)}[kT]) \\ &= \sum_s (x^s[kT] - x^{s(*)}) U_s'(\zeta) + \sum_r q_r[kT] (x_r^{s(*)} - x_r^{s(*)}[kT]) \\ &= \sum_r (x_r^s[kT] - x_r^{s(*)}) (U_s'(\zeta) - q_r[kT]) \end{aligned} \quad (29)$$

where there exists $\zeta \in (x^s[kT], x^{s(*)})$ satisfying the above expression.

We then calculate the expression $E\{\Delta \psi(\mathbf{p}[kT])\}$ for each sub-path r of (29). $U_s'(\cdot)$ is a decreasing function. Analyzing the first term of the second line in (29), if $x^{s(*)} \leq x^s[kT]$, then $U_s'(x^s[kT]) \leq U_s'(\zeta) \leq U_s'(x^{s(*)})$; If $x^s[kT] \leq x^{s(*)}$, then $U_s'(x^{s(*)}) \leq U_s'(\zeta) \leq U_s'(x^s[kT])$. Thus, we have

$$E\{\Delta \psi(\mathbf{p}[kT])\}_r \geq (U_s'(x^s[kT]) - q_r[kT]) (x_r^s[kT] - x_r^{s(*)})$$

Substituting $x_r^s[kT] = x_r^s[(k-1)T] + \dot{x}_r^s[kT]$ for $U_s'(x_r^s[kT])$, and then using the mean value theorem and (4), yields

$$\begin{aligned} E\{\Delta \psi(\mathbf{p}[kT])\}_r & \geq (U_s'(x^s[(k-1)T]) - q_r[kT] + U_s''(\xi) \dot{x}_r^s[kT]) (x_r^s[kT] - x_r^{s(*)}) \\ &= \dot{x}_r^s[kT] \left(\frac{1}{\gamma_r} + U_s''(\xi) \right) (x_r^s[kT] - x_r^{s(*)}) \\ & \geq \eta_r (x_r^s[kT] - x_r^s[(k-1)T]) (x_r^s[kT] - x_r^{s(*)}) \end{aligned}$$

where there exists $\xi \in (x^s[(k-1)T], x^s[kT])$ satisfying the above expression, then let $U_s''(\xi)$ equal to $U_{s,\min}''$. It is possible to find a suitable γ_r , satisfying $(1/\gamma_r + U_{s,\min}'') > 0$. However, it should be noted that the condition is not a tight constraint. Multiplying every term of the above expression, yields

$$E\{\Delta \psi(\mathbf{p}[kT])\}_r \geq \eta_r \{ (x_r^s[kT])^2 - x_r^s[kT] x_r^s[(k-1)T] - x_r^{s(*)} \dot{x}_r^s[kT] \} \quad (30)$$

Because (30) holds for every scheduling cycle and sub-path r , summing over all cycles in $\{1, 2, 3, \dots, M\}$, yields

$$\sum_{\tau=1}^M E\{\Delta\psi(\mathbf{p}[\tau T])\} \geq \sum_r \eta_r \sum_{\tau=1}^M \{(x_r^s[\tau T])^2 - x_r^s[\tau T]x_r^s[(\tau-1)T] - x_r^{s(*)} \dot{x}_r^s[\tau T]\}$$

Expanding the above expression, then substituting $(x_r^s[kT])^2 + (x_r^s[(k-1)T])^2 - 2x_r^s[kT]x_r^s[(k-1)T] = (\dot{x}_r^s[kT])^2$, and rearranging the expression, yields

$$\begin{aligned} \sum_{\tau=1}^M E\{\Delta\psi(\mathbf{p}[\tau T])\} &\geq \frac{1}{2} \sum_r \alpha_r \{(x_r^s[MT])^2 + (\dot{x}_r^s[MT])^2 + (\dot{x}_r^s[(M-1)T])^2 + \dots + (\dot{x}_r^s[2T])^2 + (x_r^s[T])^2 - 2x_r^{s(*)}(x_r^s[MT] - x_r^s[T])\} \\ &\geq - \sum_r \eta_r x_r^{s(*)} (x_r^s[MT] - x_r^s[T]) \end{aligned}$$

so (28) follows. ■

Lemma 2: The MAC scheduling control function satisfies

$$\phi(\mathbf{p}[kT]) \geq \sum_l p_l[kT] \sum_{r|l} (x_r^{s(*)} + \varepsilon) - \Delta\mathcal{C}(T) \quad (31)$$

where ε is a small positive number.

Proof: Since in any scheduling cycle, the network will converge to stability. According to the Proposition 2, we have

$$\sum_l p_l[kT] c_l^{(e)}[kT] \geq \sum_l p_l[kT] c_l^{(*)} - \Delta\mathcal{C}(T)$$

It is impossible to empirically inject a flow rate into a link to be greater than the link rate. Thus, we have

$$c_l^{(*)} \geq \sum_{r|l} (x_r^{s(*)} + \varepsilon)$$

so (31) follows. ■

Lemma 3: Let $x_r^{s(opt)}$ and $\mathbf{p}^{(opt)} = \{p_1^{(opt)}, p_2^{(opt)}, p_3^{(opt)}, \dots, p_{|\mathcal{L}|}^{(opt)}\}$ denotes the flow rate and Lagrange multiplier based centralized optimal scheduling. The utility based on C-MWS is upper bounded. Specifically,

$$\sum_s U_s(x^s) \leq \sum_s U_s(x^{s(opt)}) - \Delta\mathcal{A}(\mathbf{p}^{(opt)}, r_{\min}, r_{\max}, \alpha) \quad (32)$$

Proof: Taking the difference between empirical utility and optimal utility, and using Lagrange mean value theorem, yields

$$\sum_s (U_s(x^s) - U_s(x^{s(opt)})) = \sum_s (x^s - x^{s(opt)}) U_s'(\zeta)$$

where there exists $\zeta \in (x^s, x^{s(opt)})$ satisfying the above expression. Since it is impossible that $x^s = x^{s(opt)}$ for all sessions in conflict network, similar to Lemma 1's proof, we have

$$\sum_s (U_s(x^s) - U_s(x^{s(opt)})) < \sum_s (x^s - x^{s(opt)}) U_s'(x^{s(opt)})$$

When the network achieves the optimal utility through centralized optimal scheduling, it is an equilibrium network. That is, $U_s'(x^{s(opt)}) = q_r^{(opt)}$. In addition, since $q_r = \sum_{l|r} p_l$, we get

$$\sum_s (U_s(x^s) - U_s(x^{s(opt)})) < \sum_l p_l^{(opt)} \sum_{r|l} x_r^s - \sum_l p_l^{(opt)} \sum_{r|l} x_r^{s(opt)}$$

It is rational to assume that the maximal usable resource on each link can always be realized by a centralized optimal scheduling, i.e., $c_l^{(opt)} = \sum_{r|l} x_r^{s(opt)}$. Thus, according to Proposition 2, we have

$$\sum_s (U_s(x^s) - U_s(x^{s(opt)})) < \sum_l p_l^{(opt)} c_l - \sum_l p_l^{(opt)} c_l^{(opt)} = -\Delta\mathcal{A}(\mathbf{p}^{(opt)}, r_{\min}, r_{\max}, \alpha)$$

so (32) follows. \blacksquare

According to (20), it should be noted that the above lemma have an implied condition, which is that when the duration of scheduling cycle is infinite.

Since all flows' rates are upper bounded by x_{\max} , the network utility is upper bounded (not necessarily tight) by U_{\max} , i.e., $\sum_s E\{U_s(x^s[kT])\} \leq U_{\max}$.

Proposition 3: A network is simply stable if it satisfies the following condition over joint optimization cycles $\{1, 2, 3, \dots, M\}$:

$$\lim_{M \rightarrow +\infty} \frac{1}{M} \sum_{\tau=1}^M \sum_l E\{p_l[\tau T]\} \leq \frac{0.5L_{\max}\gamma_l(f_{\max}x_{\max})^2 + \Delta\mathcal{C}(T) + U_{\max}}{\varepsilon}, \quad (33)$$

furthermore, the time average utility of such a network (i.e., the expression in the middle line, see below) meets the following bounds:

$$\begin{aligned} \sum_s U_s(x^{s^{(*)}}) - (\Delta\mathcal{C}(T) + 0.5L_{\max}\gamma_l(f_{\max}x_{\max})^2) &\leq \lim_{M \rightarrow +\infty} \frac{1}{M} \sum_{\tau=1}^M \sum_s E\{U_s(x^s[\tau T])\} \\ &< \sum_s U_s(x^{s^{(opt)}}) - \Delta\mathcal{A}(\mathbf{p}^{(opt)}, r_{\min}, r_{\max}, \alpha) \end{aligned} \quad (34)$$

where $\Delta\mathcal{A}$ and $\Delta\mathcal{C}$ have been defined in (18) and (22), respectively.

Proof: Summing the Lyapunov drift with utility function over all cycles, and then taking expectation over the distribution of $\mathbf{p}[\tau T]$, the result is represented by Δ .

$$\Delta = E\{L(\mathbf{p}[MT])\} - E\{L(\mathbf{p}[T])\} - 2\gamma_l \sum_{\tau=1}^M E\left\{\sum_s U_s(x^s[\tau T])\right\} \leq M\Delta\mathcal{B} - 2\gamma_l \sum_{\tau=1}^M E\{\psi(\mathbf{p}[\tau T])\} - 2\gamma_l \sum_{\tau=1}^M E\{\phi(\mathbf{p}[\tau T])\}$$

Substituting the result of Lemma 1 and that of Lemma 2 and rearranging the expression, yields

$$\Delta \leq M(2\gamma_l\Delta\mathcal{C}(T) + \Delta\mathcal{B}) - 2\gamma_l\Delta\mathcal{D} - 2\gamma_lM \sum_s U_s(x^{s^{(*)}}) - 2\gamma_l\varepsilon M \sum_l E\{p_l[kT]\}$$

Taking the limit over M for $\sum_l E\{p_l[kT]\}$, (33) is proved. Taking the limit over M for $\sum_s E\{U_s(x^s[kT])\}$, and according to the result of Lemma 3, so (34) follows. \blacksquare

It can be seen that the lower bound of time average utility is decided by the value of expression $\Delta\mathcal{C}(T) + 0.5L_{\max}\gamma_l(f_{\max}x_{\max})^2$, where the first term decreases with increase of T , the second term decreases with decrease of γ_l . That means the lower bound is tight. According to Lemma 3, the realization of the upper bound have an implied condition (i.e., $T = \infty$). More importantly, the upper bound is decided by $\Delta\mathcal{A}(\mathbf{p}^{(opt)}, r_{\min}, r_{\max}, \alpha)$. When the network topology, flow route(s), r_{\min} , r_{\max} , and α are determined, the upper bound is determined. Furthermore, according to the proof of Lemma 3, we can conclude that the difference between the upper bound of utility and average empirical utility is decided by the relationship between x^s and $x^{s^{(opt)}}$ for each session s . Specifically, when x^s is far from $x^{s^{(opt)}}$, the average empirical utility is far from its utility upper bound; when x^s approaches to $x^{s^{(opt)}}$, $\forall s$, the average empirical utility approaches to the maximal utility upper bound. Thus, we can use the maximal upper bound of utility to evaluate whether the current C-MWS parameter setting (r_{\min} , r_{\max} and α) are optimal. Although the upper bound is not perfectly tight, the simulation results shown later show that the derived upper bound is very tight.

Furthermore, it is seen that empirical utility approaches to the maximal utility upper bound (34) as the C-MWS parameters are tuned to approach their optimal values. That is, before actual flow assignment, we can use simulation based on centralized optimal scheduling and Eq. (34) to tune the C-MWS parameters to find near-optimal utility.

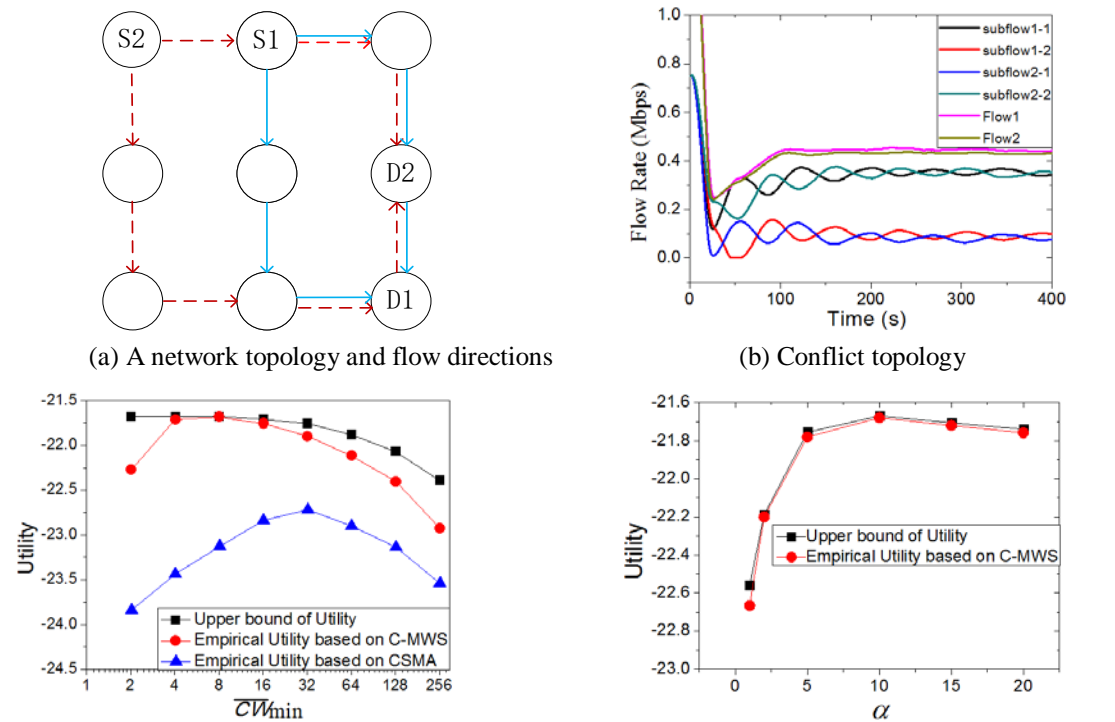
5. Numerical Results

In this section, extensive simulations were conducted to evaluate the accuracy and performance of our model and the C-MWS algorithm under different parameters including T , α , θ_{\min} , and θ_{\max} . For fairness in terms of resource allocation, we let the utility function follows a form of $U_s(x^s) = (x^s)^{(1-\omega)}/(1-\omega)$, where $\omega=1.1$. We assume the joint optimization parameters as follows: The step size of congestion control $\gamma_c = 0.1$ and that for scheduling $\gamma = 0.01$. In our simulations, each node independently works for channel access based on given C-MWS parameters. The link capacity $C_{l,\max}$ is 1Mbps, the mean transmission time for a packet is 10ms. The duration of a mini-slot (MTS) for back-off is 50us.

In the simulations, we also realized the standard CSMA (CSMA) for medium access [20] for comparison purpose. To be fair, in the implementation of standard CSMA, the assumptions made in Section 1 (i.e., 1) non-existence of hidden nodes in the network and 2) instantaneous channel sensing) are also assumed to hold. Also, when realizing the standard CSMA, we also implemented the same congestion control algorithm as used for C-MWS for flow control. In addition, we set the initial contention window size for standard CSMA to \overline{CW}_{\min} , and set its maximum backoff stage to 6.

5.1 3x3 network

Fig. 1(a) shows a 3x3 grid network and flow directions for simulations. We assume that there are two sessions in the network. Sessions 1 and 2 are from source nodes S1 and S2 to destination nodes D1 and D2, respectively, where the two sub-paths for session 1 are represented by blue solid line, and those for session 2 are shown in red dotted line.



(c) Utility upper bound and empirical utility vs \overline{CW}_{\min} (d) Utility upper bound and empirical utility vs α

Fig. 1. Numerical results for 3 x 3 Network.

In the first test, $\overline{CW}_{\max} = 1024$, $\overline{CW}_{\min} = 8$, $\alpha = 10$, and $T = 0.8s$. **Fig. 1(b)** shows the convergence of flow rates. It can be seen that the flow rate for each session converge to a small range.

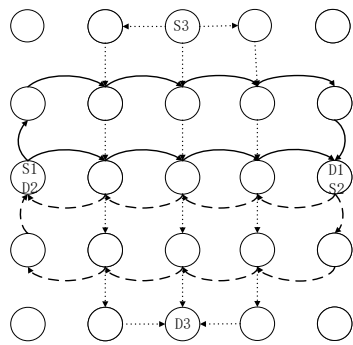
In the second test, we compare the upper bound of utility derived by (34) with the empirical utility obtained via simulations. In this test, $T = 0.8s$, and $\overline{CW}_{\max} = 1024$. **Fig. 1(c)** shows how the utility changes with \overline{CW}_{\min} when $\alpha = 10$. In **Fig. 1(c)**, it can be seen that both utility upper bound and empirical utility based on C-MWS reach the maximum when $\overline{CW}_{\min} = 8$. Note that there exists insignificant difference between the theoretical upper bound and the empirical utility based on C-MWS when $\overline{CW}_{\min} = 8$ because of the finiteness of T and near-optimality of C-MWS parameters. However, in standard CSMA, channel accessing by different links has not considered their queueing sizes (resulted by the flow assignment/control algorithm at the transport layer), and the resulting empirical utility by standard CSMA is thus significantly lower than that by C-MWS. **Fig. 1(d)** shows how the utilities change with α when $\overline{CW}_{\min} = 8$ and $T = 0.8s$. In **Fig. 1(d)**, it is seen that the utility reaches the maximum when $\alpha = 10$.

Fig. 1(c) shows that the upper bound is a non-increasing function of \overline{CW}_{\min} . The reason is as follows. According to Proposition 1, by using (14), we can obtain the maximal weighted link capacities when \overline{CW}_{\min} is very small because in this case it has negligible impact on the per-link TA by (17). With the increase of \overline{CW}_{\min} , the weighted link capacity by (14) decreases due to the increase of r_{\max} in (17). Furthermore, it can be clearly seen that the upper bound by (34) is positively correlated to the weighted network capacity by (14). Thus, we can obtain that the upper bound is a non-increasing function of \overline{CW}_{\min} . In addition, in **Fig. 1(c)**, it is seen that the empirical utility based on C-MWS scheduling is very close to the utility upper bound when appropriate parameters are chosen, thus, we can say that the upper bound is very tight and that the empirical utility is very close to the maximal network utility in this case because the upper bound $>$ maximal network utility $>$ empirical utility based on C-MWS.

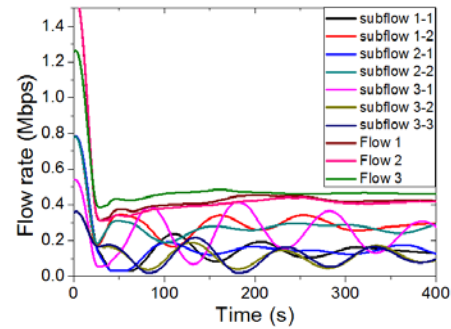
5.2 5×5 network

Fig. 2(a) shows a more complex 5×5 grid network and three sessions, where sessions 1, 2, and 3 have 2, 2, and 3 sub-paths from their source nodes to destination nodes, respectively. In this topology, there are 36 directional links involved. These links can construct 4956 mutually non-included independent sets and more than one hundred thousand independent sets in total. Assume $\overline{CW}_{\max} = 1024$, $\overline{CW}_{\min} = 16$, $\alpha = 30$, and $T = 0.8s$, **Fig. 2(b)** shows the convergence of flow rates of different sessions and sub-paths.

In the test, we calculate the upper bound of utility by (34) based on various independent sets. Setting $T = 0.8s$, and $\overline{CW}_{\max} = 1024$. **Fig. 2(c)** shows how the utility changes with \overline{CW}_{\min} when $\alpha = 30$. **Fig. 2(c)** shows that empirical utility based on C-MWS reaches the maximum, and the gap between the theoretical upper bound and the empirical utility based on C-MWS reaches the minimum when $\overline{CW}_{\min} = 16$. Since the 5×5 network has more channel conflicts than the 3×3 network in the preceding subsection, the optimal C-MWS parameter (\overline{CW}_{\min}) for the former is larger than its counterpart for the latter. Again, in **Fig. 2(c)**, it can be clearly seen that the utility by standard CSMA is much lower than that by C-MWS. **Fig. 2(d)** shows how the utilities change with α when $\overline{CW}_{\min} = 16$. **Fig. 2(d)** shows that the utility reaches the maximum when $\alpha = 30$. Again, **Fig. 2(c)** shows that the upper bound is very tight when appropriate parameters are chosen and also the empirical utility based on C-MWS can achieve near-optimal network utility when related parameters are well tuned.



(a) 5×5 network and flow directions



(b) Flow rate

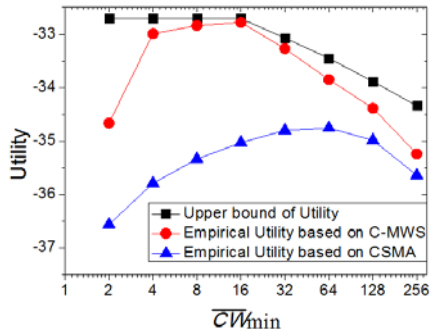
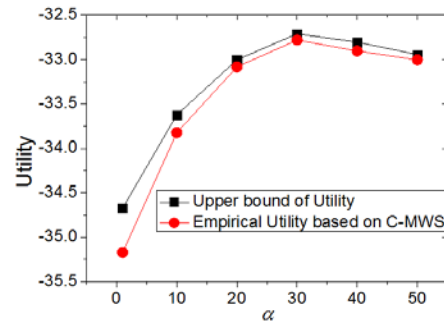
(c) Utility upper bound and empirical utility vs \overline{CW}_{min} (d) Utility upper bound and empirical utility vs α

Fig. 2. Numerical results for 5 × 5 Network.

6. Conclusion

In this paper, we extended traditional continuous time Markov model by discretizing the network time and modeled the weighted network capacity for CSMA wireless networks with consideration of channel conflict. We further proposed a C-MWS algorithm for achieving this capacity and discussed how to tune its parameters. We proved the network stability under our model and C-MWS, and derived lower and upper bounds of corresponding network utility. Simulation results showed that the joint optimization based on C-MWS can achieve near-optimal network utility when appropriate parameters are chosen, and the derived utility upper bound is very tight.

References

- [1] Mung Chiang, Steven H. Low, Robert A. Calderbank, and John C. Doyle, "Layering as optimization decomposition - A mathematical theory of network architectures," in *Proc. of the IEEE*, vol. 95, no. 1, pp. 255-312, January 2007. [Article \(CrossRef Link\)](#)
- [2] Steven H. Low and David E. Lapsley, "Optimization Flow Control, I: Basic Algorithm and Convergence," *IEEE/ACM Transactions on Networking*, vol. 7, no. 6, pp. 861-874, December 1999. [Article \(CrossRef Link\)](#)
- [3] Xiaojun Lin, Ness B. Shroff, and R. Srikant, "On the connection-level stability of congestion-controlled communication networks," *IEEE Transactions on Information Theory*, vol. 54, no. 5, pp. 2317-2338, May 2008. [Article \(CrossRef Link\)](#)

- [4] Roberto Cominetti and Cristobal Guzmán, “Network congestion control with Markovian multipath routing,” *Mathematical Programming*, vol. 147, no. 1, pp. 231-251, October 2014. [Article \(CrossRef Link\)](#)
- [5] Andres Ferragut and Fernando Paganini, “Network Resource Allocation for Users With Multiple connections fairness and stability,” *IEEE/ACM Transactions on Networking*, vol. 22, no. 2, pp. 349-362, April 2014. [Article \(CrossRef Link\)](#)
- [6] Jang-Won Lee, Mung Chiang, and Robert A. Calderbank, “Jointly optimal congestion and medium access control in ad hoc wireless,” in *Proc. of IEEE 2006 Vehicular Technology Conference (VTC’06)*, pp. 284-288, May 2006.
- [7] Xin Wang and Koushik Kar, “Cross-layer rate optimization for proportional fairness in multihop wireless networks with random access,” *IEEE Journal on Selected Areas in Communications*, vol. 24, no. 8, pp. 1548-1559, August 2006. [Article \(CrossRef Link\)](#)
- [8] Atilla Eryilmaz and R. Srikant, “Joint Congestion Control, Routing and MAC for stability and fairness in wireless networks,” *IEEE Journal on Selected Areas in Communications*, vol. 24, no. 8, pp. 1514-1524, August 2006. [Article \(CrossRef Link\)](#)
- [9] Michael J. Neely, Eytan Modiano, and Chih-Ping Li, “Fairness and optimal stochastic control for heterogeneous networks,” *IEEE/ACM Transactions on Networking*, vol. 16, no. 2, pp. 396-409, Apr. 2008. [Article \(CrossRef Link\)](#)
- [10] Peng Wang and Stephan Bohacek, “Practical Computation of Optimal Schedules in Multihop Wireless Networks,” *IEEE/ACM Transactions on Networking*, vol. 19, no. 2, pp. 305-318, April 2011. [Article \(CrossRef Link\)](#)
- [11] Libin Jiang and Jean Walrand, “A Distributed CSMA Algorithm for Throughput and Utility Maximization in wireless networks,” *IEEE/ACM Transactions on Networking*, vol. 18, no. 3, pp. 960-972, June 2010. [Article \(CrossRef Link\)](#)
- [12] Jiaping Liu, Yung Yi, Alexandre Proutierel, Mung Chiang, and H. Vincent Poort, “Convergence and Tradeoff of Utility-Optimal CSMA,” in *Proc. of Broadband Communications, Networks, and Systems Conference*, pp. 1-8, September 2009. [Article \(CrossRef Link\)](#)
- [13] Libin Jiang and Jean Walrand, “Approaching Throughput-Optimality in a Distributed CSMA Scheduling Algorithms with Collisions,” *IEEE/ACM Transactions on Networking*, vol. 19, no. 3, pp. 816-829, June 2011. [Article \(CrossRef Link\)](#)
- [14] Caihong Kai and Shengli Zhang, “Throughput Analysis of CSMA Wireless Networks with Finite Offered-load,” in *Proc. of IEEE 2013 International Conference on Communications (ICC’13)*, pp. 6101-6106, June 2013. [Article \(CrossRef Link\)](#)
- [15] Hyeryung Jang, Se-Young Yun, Jinwoo Shin, and Yung Yi, “Distributed Learning for Utility Maximization over CSMA-based Wireless Multihop Networks,” in *Proc. of IEEE International Conference on Computer Communications (INFOCOM’14)*, pp. 280-288, May 2014. [Article \(CrossRef Link\)](#)
- [16] Jian Ni, Bo Tan, and R. Srikant, “Q-CSMA: Queue-Length-Based CSMA/CA Algorithms for Achieving Maximum Throughput and Low Delay in Wireless Networks,” *IEEE/ACM Transactions on Networking*, vol. 20, no. 3, pp. 825-836, June 2012. [Article \(CrossRef Link\)](#)
- [17] Se-Young Yun, Jinwoo Shin, and Yung Yi, “CSMA over time-varying channels: optimality, uniqueness and limited backoff rate,” in *Proc. of ACM 2013 International symposium on Mobile ad hoc networking and computing (MobiHoc’13)*, pp. 137-146, July 2013. [Article \(CrossRef Link\)](#)
- [18] Jin-Ghoo Choi, Changhee Joo, Junshan Zhang, and N. B. Shroff, “Distributed Link Scheduling Under SINR Model in multihop wireless networks,” *IEEE/ACM Transactions on Networking*, vol. 22, no. 4, pp. 1204-1217, August 2014. [Article \(CrossRef Link\)](#)
- [19] Michael J. Neely, Eytan Modiano, and Charles E. Rohrs, “Dynamic Power Allocation and Routing for time varying wireless networks,” *IEEE Journal on Selected Areas in Communications*, vol. 23, no. 1, pp. 98-103, January 2005. [Article \(CrossRef Link\)](#)
- [20] Giuseppe Bianchi, “Performance analysis of the IEEE 802.11 distributed coordination function,” *IEEE Journal on Selected Areas in Communications*, vol. 18, no. 3, pp. 535-547, March 2000. [Article \(CrossRef Link\)](#)

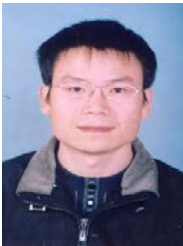
- [21] Bruno Nardelli and Edward W. Knightly, "Closed-form throughput expressions for CSMA networks with collisions and hidden terminals," in *Proc. of IEEE 2012 International Conference on Computer Communications (INFOCOM'12)*, pp. 2309-2317, March 2012. [Article \(CrossRef Link\)](#)
- [22] Beakcheol Jang and Mihail. L. Sichitiu, "IEEE 802.11 Saturation Throughput Analysis in the Presence of Hidden Terminals," *IEEE/ACM Transactions on Networking*, vol. 20, no. 2, pp. 557-570, April 2012. [Article \(CrossRef Link\)](#)
- [23] Nikolaos M. Freris, "Performance bounds for CSMA-based Medium Access Control," in *Proc. of IEEE Decision and Control and European Control Conference (CDC-EDC'11)*, pp. 5945-5950, December 2011. [Article \(CrossRef Link\)](#)
- [24] Sankrith Subramanian, Eduardo L. Pasiliao, John M. Shea, Jess W. Curtis, and Warren E. Dixon, "Throughput Maximization in CSMA Networks with Collisions and Hidden Terminals," *Springer Proceedings in Mathematics and Statistics*, pp. 195-205, July 2012.
- [25] Soung Chang Liew, Cai Hong Kai, Hang Ching Leung, and Piu Wong, "Back-of-the-envelope computation of throughput distributions in CSMA wireless networks," *IEEE Transactions on Mobile Computing*, vol. 9, no. 9, pp. 1319-1331, May 2010. [Article \(CrossRef Link\)](#)
- [26] Xin Wang and Koushik Kar, "Throughput Modelling and Fairness Issues in CSMA/CA Based Ad-Hoc Networks," in *Proc. of IEEE 2005 International Conference on Computer Communications (INFOCOM'05)*, pp. 23-31, March 2005.
- [27] F.P. Kelly, *Reversibility and Stochastic Networks*, Wiley, 1979.
- [28] Libin Jiang and Jean Walrand, "Convergence and Stability of a Distributed CSMA Algorithm for Maximal Network Throughput," *Technical Report*, University of California at Berkeley, March 2009. [Article \(CrossRef Link\)](#)



Tao Wang is currently pursuing his Ph.D. degree in computer science at Research Center of Ubiquitous Sensor Networks at the University of Chinese Academy of Science (UCAS), Beijing, China. He received his BS degree and MS degree in automation engineering from Central South University and Tianjin University, China, respectively, in 2007 and 2009. He worked as a wireless communication engineer in Huaxin Consulting Co., Ltd., China, from 2009 to 2011, and in Huawei Technologies Co., Ltd., China, from 2012 to 2013, respectively. His research interests include design of cross-layer optimization and scheduling algorithm in wireless sensor and ad hoc networks.



Zheng Yao received his B.S. degree in Computer Science and Engineering from Xi'an Jiaotong University in 1991, and received his MS and Ph.D degree in Computer Application from Harbin Institute of Technology, China, in 1994 and 1997, respectively. He is currently a Full Professor with Research Center of Ubiquitous Sensor Networks, University of Chinese Academy of Sciences. He has published over 20 papers in archival journals and conference proceedings. His research interests covers software engineering, open source software, wireless sensor networks, and Internet of Things.



Baoxian Zhang received his PhD degree in Communications & Information Systems from Northern Jiaotong University, China, in 2000. He is currently a Full Professor with the Research Center of Ubiquitous Sensor Networks at the University of Chinese Academy of Sciences (UCAS), Beijing, China. Prior joining UCAS, he was a Research Scientist with School of Information Technology and Engineering, University of Ottawa, Canada from 2002 to 2005. From 2001 to 2002, he was a Postdoctoral Fellow with Department of Electrical and Computer Engineering, Queen's University, Kingston, Canada. He is currently an Associate Editor of *IEEE Systems Journal* and had served as Guest Editors of several special issues including *IEEE Journal on Selected Areas in Communications* and *Elsevier Ad Hoc Networks Journal*. He has served on technical program committees for many international conferences and symposia. He has published over 150 refereed technical papers in archival journals and conference proceedings. His research interests cover network protocol and algorithm design, wireless ad hoc and sensor networks, Internet of Things, IP networks. Dr. Zhang is a senior member of the IEEE (2012).



Cheng Li received the B. Eng. and M. Eng. degrees from Harbin Institute of Technology, Harbin, P. R. China, in 1992 and 1995, respectively, and the Ph.D. degree in Electrical and Computer Engineering from Memorial University, St. John's, Canada, in 2004. He is currently a Full Professor at the Faculty of Engineering and Applied Science of Memorial University, St. John's, Canada. His research interests include mobile ad hoc and wireless sensor networks, wireless communications and mobile computing, switching and routing, and broadband communication networks. He is an editorial board member of *Wiley Wireless Communications and Mobile Computing* and *Journal of Networks*, and an associate editor of *Wiley Security and Communication Networks*. He has served as a co-chair for various technical symposia of many international conferences, including the IEEE GLOBECOM and ICC. He has served as the TPC member for many international conferences, including the IEEE ICC, GLOBECOM, and WCNC. Dr. Li is a registered Professional Engineer (P. Eng.) in Canada and is a Senior Member of the IEEE and a member of the IEEE Communication Society, Computer Society, Vehicular Technology Society, and Ocean Engineering Society.